Edge effects enhance carbon uptake and its vulnerability to climate change in temperate broadleaf forests

Andrew B. Reinmann[a,1] and Lucy R. Hutyra[a]

[a]Department of Earth and Environment, Boston University, Boston, MA 02215

Edited by Oskar Franklin, International Institute for Applied Systems Analysis, Laxenburg, Austria, and accepted by Editorial Board Member Gregory P. Asner November 16, 2016 (received for review July 26, 2016)

Forest fragmentation is a ubiquitous, ongoing global phenomenon with profound impacts on the growing conditions of the world's remaining forest. The temperate broadleaf forest makes a large contribution to the global terrestrial carbon sink but is also the most heavily fragmented forest biome in the world. We use field measurements and geospatial analyses to characterize carbon dynamics in temperate broadleaf forest fragments. We show that forest growth and biomass increase by 89 ± 17% and 64 ± 12%, respectively, from the forest interior to edge, but ecosystem edge enhancements are not currently captured by models or approaches to quantifying regional C balance. To the extent that the findings from our research represent the forest of southern New England in the United States, we provide a preliminary estimate that edge growth enhancement could increase estimates of the region's carbon uptake and storage by 13 ± 3% and 10 ± 1%, respectively. However, we also find that forest growth near the edge declines three times faster than that in the interior in response to heat stress during the growing season. Using climate projections, we show that future heat stress could reduce the forest edge growth enhancement by one-third by the end of the century. These findings contrast studies of edge effects in the world's other major forest biomes and indicate that the strength of the temperate broadleaf forest carbon sink and its capacity to mitigate anthropogenic carbon emissions may be stronger, but also more sensitive to climate change than previous estimates suggest.

climate change | forest fragmentation | land cover change | terrestrial carbon cycle | tree growth

Despite advances in measurement and remote sensing methods for carbon (C) accounting, considerable uncertainty remains in estimates of the global forest C sink and the C implications of deforestation (1–4). Expansion of agricultural and developed land has reduced global forest cover by one-third (5) and led to emissions of up to 146 Pg C to the atmosphere since 1850 (3). These changes in land cover and land use have also resulted in widespread landscape fragmentation, with 20% of the world's remaining forest within 100 m of a forest's edge (6). Compared with the forest interior, forest edges often experience altered growing conditions because of novel microenvironment conditions that typically include higher temperatures, vapor pressure deficit, wind, and availability of resources, such as light and nutrients (7–10). Consequently, the effects of deforestation on the terrestrial C cycle extend into adjacent forest fragments (10–12), with a growing body of research from tropical rainforests (10), temperate rainforests (11), and boreal forests (12) showing widespread increases in tree mortality and reductions in biomass near the forest's edge. Edges were recently associated with a 10% reduction in tropical forest C density (13), which highlights the importance of considering landscape fragmentation when quantifying regional C balance (14). Furthermore, the potential for forest edge effects to exacerbate forest response to climate extremes (15) confounds conventional understanding of feedbacks between the terrestrial C cycle and climate. Although C cycle–climate feedback models, which play a crucial role in projecting future climate, are becoming increasingly sophisticated and consider the direct effects of deforestation on the terrestrial C cycle, lack of sufficient empirical data precludes parameterization necessary to capture edge effects.

In light of the globally important implications of extensive and ongoing forest fragmentation for ecosystem processes, quantitative characterization of the effects of fragmentation on forest growth and its response to climate is essential for constraining forest C balance and climate projections. The temperate broadleaf forest has a C sink equivalent to ∼60% of the global net forest sink (1) and is the most heavily fragmented (6) forest biome in the world. However, although it is also one of the most heavily studied ecosystems, the effects of fragmentation on temperate broadleaf forest growth and C storage and its sensitivity to climate remain poorly understood.

This study quantifies the edge effect on forest growth and C storage in temperate broadleaf forests using data collected from forest fragments in Massachusetts, United States. We focus on forests dominated by oak species (*Quercus* spp.), because they are the most common forest types (Fig. S1), and oaks are the most common tree genus in North America's more than 130 Mha temperate broadleaf forest (16, 17). Across a series of plots 20-m wide and extending 30 m from the forest's edge to its interior, we quantified the basal area (BA; i.e., cross-sectional area of wood),

Significance

A large proportion of the world's forest is highly fragmented, but our understanding of forest carbon dynamics and their response to climate largely comes from unfragmented forests, which presents an important mismatch between landscapes that we study and those that we aim to characterize. We find that temperate broadleaf forest growth and biomass in southern New England increase substantially from forest interior to edge. However, forest growth reductions with climate stress increase with proximity to the edge, pointing to important interactions between forest fragmentation and climate change. We show that, by not accounting for edge effects, current approaches to quantifying regional and global carbon balance may underestimate carbon sequestration and not accurately represent forest growth response to future climate change.

Author contributions: A.B.R. and L.R.H. designed research, performed research, analyzed data, and wrote the paper.

The authors declare no conflict of interest.

This article is a PNAS Direct Submission. O.F. is a Guest Editor invited by the Editorial Board.

Freely available online through the PNAS open access option.

Data deposition: The data reported in this paper are available at Dataverse, https://dataverse.harvard.edu/citation?persistentId=doi:10.7910/DVN/AZGSQV.

[1]To whom correspondence should be addressed. Email: reinmann@bu.edu.

This article contains supporting information online at www.pnas.org/lookup/suppl/doi:10.1073/pnas.1612369114/-/DCSupplemental.

tree growth rates, and soil properties. We use soil and coarse woody debris (CWD) data, BA, and basal area increment (BAI; i.e., annual wood increment) in a linear mixed effects model framework to quantify relative changes in C storage and growth from the forest's interior to edge. Tree core analysis indicates that forest age in the plots used for this study ranges from 61 to 84 y, which is similar to 60% of forests in southern New England (Fig. S1). All forest edges were created more than 30 y ago, and we used historical climate records to isolate climate drivers of interannual variability in tree and forest growth.

Results and Discussion

Forest Growth and C Storage. We find that forest edge effects substantially enhance aboveground forest growth and C storage. The forest BAI (hereafter "forest growth") and BA increase by 89 ± 17% ($P < 0.001$) and 64 ± 12% ($P < 0.001$), respectively, from the forest's interior (20- to 30-m segment) to edge (0- to 10-m segment) (Fig. 1). Oaks make up 74.8 ± 7.1% of the BA in our plots (Fig. 1) and a plurality (35%) of the forest biomass in southern New England (18). Oak relative BA varied across plots, but we find no significant effect of species composition on the magnitude of forest growth response to edge effects ($P > 0.40$) (Table S1). Furthermore, there is no discernable effect of solar aspect on the pattern or magnitude of the forest growth and C storage response to edge effects ($P = 1$). Increased light availability near forest edges is likely an important mechanism driving the observed increase in forest growth, analogous to increases in tree growth after precommercial thinning treatments used by silviculturists and foresters. Oak radial growth has been shown to nearly double after even low levels of thinning (19). Similarly, research across 91 sites in Massachusetts indicates that radial growth rates of individual oak trees nearly double after the clearing of adjacent land for development (20). Although overall forest growth consistently increases with proximity to the edge, we find that the growth response of individual trees varies with patterns in tree stem density. In forests where stem density increases with proximity to the edge, the growth rate of individual trees generally remains constant, whereas in forest stands where stem density does not vary across the plot, the growth rate of individual trees generally increases (Fig. S2); each mechanism results in higher overall forest growth. Although previous work in temperate forest fragments has focused on either growth of individual trees (21) or tree stem density (22), our findings suggest that neither metric alone provide a good proxy for growth at the forest scale.

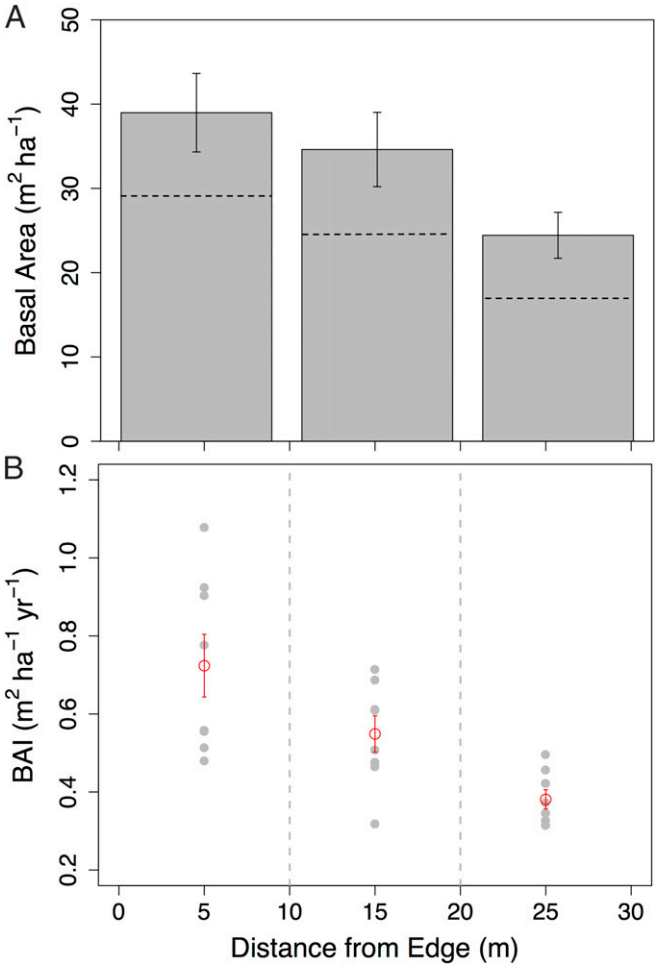

Fig. 1. Response of forest biomass and growth to forest edge effects. (*A*) Total BA (gray bars) and contribution from oak trees (dashed lines) with distance from the forest's edge averaged across plots (slope = −7.275; $P < 0.001$). (*B*) Forest BAI (2005–2014 mean) with distance from the forest's edge (slope = −0.1713; $P < 0.001$) for each plot (gray circles; $n = 8$ for each forest segment) and means of all plots (red circles). Error bars represent SEM.

In contrast to the aboveground processes, analyses of eight soil samples from each plot suggest that total C and N content and root biomass in the top 10 cm of the soil do not vary with proximity to the forest's edge ($P > 0.05$). Similarly, from a series of seven 20-m-long transects in each plot, we observe no patterns in CWD between the forest's interior and edge ($P = 0.13$), suggesting that, in contrast to other forest types (10–12), fragmentation might not increase rates of tree turnover in temperate broadleaf forests.

Edge Effects on Climate Sensitivity of Forest Growth. Although forest growth is consistently higher near the forest's edge than in the interior, the magnitude of this edge enhancement varied with annual climate. We find that interannual variability in forest growth more than doubles with proximity to the forest's edge from a range of 0.28 ± 0.04 $m^2\ ha^{-1}\ y^{-1}$ in the forest's interior to a range of 0.58 ± 0.12 $m^2\ ha^{-1}\ y^{-1}$ in the 0- to 10-m forest segment (Fig. 2 and Fig. S3). Heat stress, defined here as the number of days in June and July above 27 °C (the July average high temperature in Boston, MA), alone explained 30% (0–10 m from forest edge) to 36% (10–20 and 20–30 m from forest edge) of the interannual variability in forest growth between 1990 and 2014 ($P < 0.01$) (Fig. 2). These findings are in agreement with earlier studies that show the adverse effects of high temperatures during early summer on growth of oak trees in the eastern United States (23) and forest net primary productivity (NPP) in New England (24). In our study, results from linear regression models indicate that declines in forest BAI in response to heat stress increase from 0.004 to 0.011 $m^2\ ha^{-1}\ y^{-1}$ for each additional day above 27 °C between the forest's interior and edge, respectively (Fig. 2).

The edge effect on climate sensitivity of forest growth suggests the potential for interactions between land cover change and climate change. To estimate a first approximation of potential changes in the forest edge growth enhancement under climate change, we used downscaled climate projections from Phase 5 of the Coupled Model Intercomparison Project (CMIP5) (Table S2) (25). These climate projections indicate that southern New England is likely to experience an average of 48.2–56.6 d above 27 °C during June and July between 2080 and 2099 under the Intergovernmental Panel on Climate Change Representative Concentration Pathway 4.5 (RCP4.5; low emissions) and RCP8.5 (high emissions) scenarios, respectively. These projections suggest that forest exposure to heat stress could nearly double (1990–2014 mean is 29 d) by the end of the 21st century, reducing forest growth by 33–42% from the forest's interior to edge under the RCP 8.5 scenario (Fig. 2).

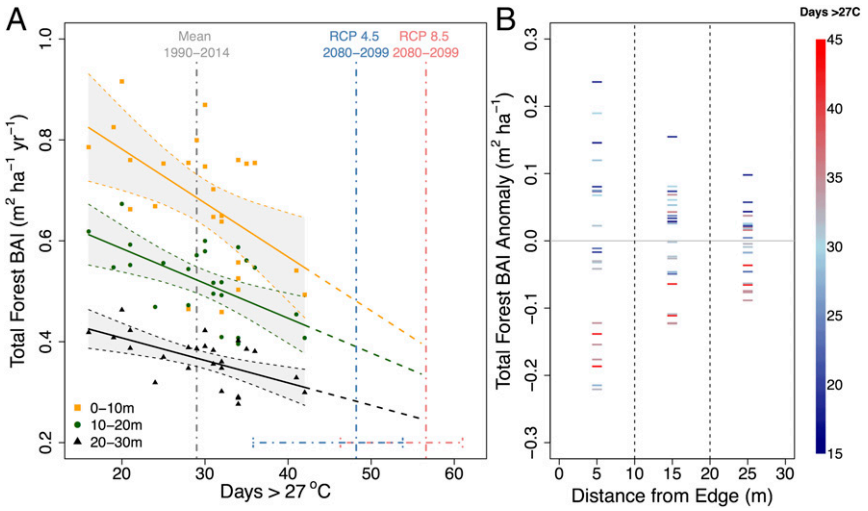

Fig. 2. Forest growth response to growing season heat stress. (*A*) Relationship between total forest BAI for 1990–2014 and heat stress (number of days in June and July with air temperature above 27 °C). Data are partitioned into segments of 0–10 (slope = −0.011; $P = 0.009$; $r^2 = 0.30$), 10–20 (slope = −0.007; $P = 0.002$; $r^2 = 0.36$), and 20–30 m (slope = −0.004; $P = 0.001$; $r^2 = 0.36$) from the forest's edge and represent means across the plots measured in this study. Gray shaded areas indicate the 95% confidence intervals. Vertical lines indicate the mean numbers of days above 27 °C for 1990–2014, 2080–2099 CMIP5 RCP4.5, and 2080–2099 CMIP5 RCP8.5. The horizontal blue and red dotted bars represent the range in the mean number of days >27 °C across the CMIP5 ensemble model runs. (*B*) Forest BAI anomaly and heat stress for each 10-m forest segment; mean forest BAI between 1990 and 2014 was used as the reference period. In each panel, $n = 25$ for each forest segment.

Regional Implications of Forest Edge Effects. We used the 2011 National Land Cover Database (NLCD) land cover maps (26) to scale up our data to southern New England (Massachusetts, Connecticut, and Rhode Island) as a first approximation of the landscape-scale implications of the forest edge effect on growth and C storage in the temperate broadleaf forest. This region of the northeastern United States includes forestland (64%) interspersed with large population centers and developed (27%) and agricultural (7%) land. Across the 2.2 million ha forest in southern New England, US Forest Inventory and Analysis (FIA) data indicate that forest NPP and aboveground C storage are 4.8 ± 0.18 Tg C y^{-1} and 179 ± 2.9 Tg C, respectively (18). However, although the FIA data (Table S3) are commonly used to quantify forest growth and C storage at regional to national scales [e.g., the work by Woodbury et al. (27)], FIA sampling was not designed to capture the effects of edges and fragmentation on forest growth and biomass. Across southern New England, 9.6% and 17.8% of the forest are within 10 and 20 m of the forest's edge, respectively (Fig. 3 and Table S3). To the extent that the plots that we studied represent forest edge growth enhancement throughout southern New England, the forest edge effect could increase aboveground growth and C storage of the 2.2 million ha forest that remains in southern New England by 13 ± 3% (0.6 Tg C y^{-1}) and 10 ± 1% (17 Tg C), respectively. Although additional research is necessary to develop robust regional estimates, these findings show the potential of the edge growth enhancement in the temperate broadleaf forest to play an important role in offsetting declines in the C sink associated with deforestation and urban development. However, our results should not be interpreted as support of fragmentation as a management strategy. Even accounting for a forest edge growth enhancement, the current regional forest C sink of southern New England is 31%

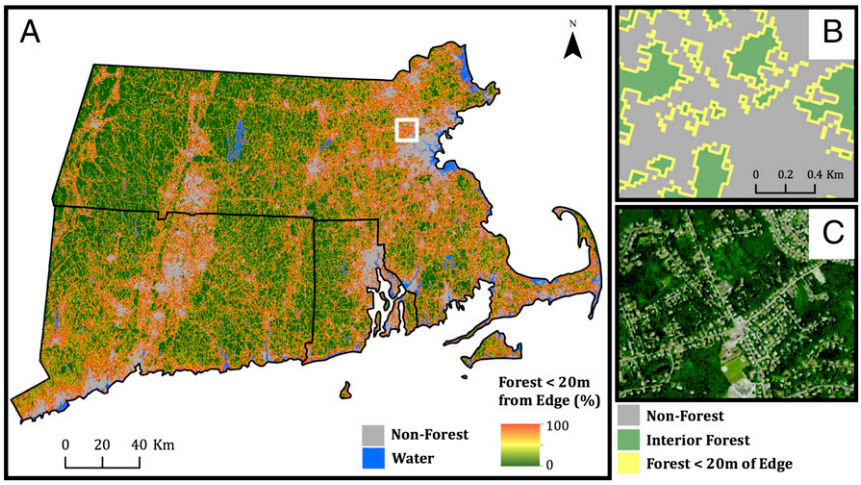

Fig. 3. (*A*) Spatial patterns in the proportion of forest within 20 m of an edge across southern New England (states outlined in black) at 100-m resolution. *B* and *C* show mapped forest fragmentation and satellite imagery (Google Earth), respectively, of the area surrounding one of our research locations in eastern Massachusetts (within the white outlined box in *A*).

lower than it would have been in the absence of the 1.4-Mha net decline in forest area since the precolonial era (28). Forest fragmentation also has many other well-documented adverse impacts on biodiversity and ecosystem services (6).

Forest age, forest type, and land cover adjacencies were not considered when scaling our plot-level data to the forests of southern New England, but these characteristics may play important roles in determining the magnitude of the forest edge growth enhancement and its response to climate. The forest fragments studied here, like the forests of southern New England and more broadly, the temperate broadleaf forest of the eastern United States, are relatively young (i.e., <100 y old) (Fig. S1). Although age-related decline in forest growth is a widely observed phenomenon, the underlying mechanisms and timing of growth decline are complicated (29), and it is unclear how the forest edge growth enhancement observed here will evolve with stand age. Growth rates of at least some broadleaf forests in southern New England have been increasing in recent decades, despite forest ages of 75–110 y (30). Furthermore, Briber et al. (20) show that individual oak trees across a wide range in size and age exhibit a strong growth enhancement after the creation of a forest edge. However, as the forests of southern New England and the eastern United States age and become more structurally complicated but also, more fragmented, understanding relationships between forest age, species composition, and edge growth enhancement will be necessary for accurate modeling of forest C balance. BA data that we collected from an additional series of plots across oak, mixed broadleaf, and mixed broadleaf/conifer forests in central and eastern Massachusetts suggest that the forest edge enhancement that we describe above for our intensively surveyed plots transcends numerous forest types (Fig. S4). However, future work should build on our findings and characterize edge effects on growth and climate sensitivity in additional forest types and regions within the temperate broadleaf forest. Additionally, the land use and land cover adjacent to a forest edge can be important drivers of forest edge microenvironment conditions by influencing variables, such as temperature (e.g., road vs. vegetated surfaces) and resource availability (e.g., irrigated and fertilized lawn or cropland vs. meadow or unamended lawn), and we suggest that the associated effects on forest growth be further explored.

Conclusions

Here, we provide a comprehensive analysis of edge effects on temperate broadleaf forest growth and C storage as well as an analysis of the importance of edge effects as a mediator of forest growth response to climate. Our findings in conjunction with earlier research (20–22) show that the paradigm describing forest edge biomass dynamics in tropical rainforests (10), temperate rainforests (11), and boreal forests (12) may not be applicable to the temperate broadleaf forest. Forest ecosystems that have exhibited edge-related declines in biomass typically have either large, tall stature trees (up to 50–60 m) or shallow roots, and these factors are commonly associated with increased wind-induced tree mortality (10–12, 31). By contrast, the modest height stature (generally <25m), deciduous nature, and relatively deep roots of trees in the temperate broadleaf forest likely bolster its resilience to increased wind exposure near the forest's edge and allow the remaining forest to capitalize on greater resource availability (e.g., light) (8). We posit that global patterns in the response of forest growth and biomass to edge effects are generally driven by a combination of increased vulnerability to disturbance (i.e., wind, drought, and fire) and an increase in light availability. Recently, an edge-related 10% decline in biomass was reported for the world's tropical forest (13), which assuming proportional declines in C uptake, would reduce the tropical forest C sink by 0.27 Pg C y^{-1} (1). By contrast, applying our estimated 13% edge enhancement on forest growth in southern New England to the world's temperate forest suggests that temperate forest edge effects could potentially offset 37% [0.10 Pg C y^{-1} (1)] of edge-related declines in the tropical forest C sink and ∼10% of global emissions from land use and land cover change (32).

Despite advances in accounting methods, there is still considerable uncertainty in estimates of the global terrestrial C sink (3, 4). Monitoring efforts, such as national forest inventory programs (e.g., US FIA) and FluxNet, have often been used to quantify C storage and rates of sequestration of US forests at regional to global scales (1, 33–35); however, these approaches were not designed to capture the effects of edges and fragmentation on forest growth and biomass and do not capture this important determinant of forest C balance and its sensitivity to climate. Consequently, current accounting methods may not capture forest C balance and its sensitivity to climate. Empirical field data (including this study) highlight the profound edge-related changes in aboveground C cycling that occur in remnant forests after fragmentation across a broad range of forest biomes. Given the continued forest fragmentation, edge effects will play an important role in constraining estimates of the terrestrial C sink and its feedback with climate.

Materials and Methods

Site Description. Field data for this study were collected from temperate broadleaf forest fragments in eastern Massachusetts, United States in the towns of Belmont (42.24° N, 71.11° W, 10 m above sea level) and Lynn (42.29° N, 70.59° W, 30 m above sea level). Eastern Massachusetts has a heterogeneous fragmented landscape consisting of forest (48% of the land area) interspersed with mostly developed (30% of land area) and agricultural land covers (10%). The climate is humid continental with warm summers and cold, snowy winters. Boston has mean maximum monthly temperatures of 2.1 °C in January and 27.4 °C in July and receives ∼1,100 mm precipitation evenly distributed throughout the year (36).

The landscape of eastern Massachusetts, similar to much of the eastern United States, was nearly entirely forest before European colonization (∼1600), but rapid agricultural expansion reduced forest cover to less than 30% of land area by the middle of the 19th century (28, 37). Agricultural abandonment in the late 19th and 20th centuries facilitated natural regeneration of the forest, which is the source of much of the region's current forest cover. The fragmented nature of the modern landscape is the product of forest fragments regenerating adjacent to maintained cropland and pastures, high road density, and urban expansion into regenerating forests. Oak species (*Quercus* spp.) are one of the most common tree genera in the region's forests, and forest canopy height is typically 15–25 m.

During the summer of 2015, we established eight plots, each 20-m wide along the forest's edge and extended 30 m into the forest's interior. Previous work in similar forests of the eastern United States showed that edge effects on forest microenvironment largely dissipate within 20 m of the edge (8), and we assume that the 20- to 30-m segment of each plot in our study is representative of the forest's interior. The forest edge of each plot was at least 30 y old; had a southern (n = 3), northern (n = 3), or eastern (n = 2) orientation; and was adjacent to either a meadow or residential development with single-family homes and yards consisting of lawns, landscaping, and ornamental trees (Table S4). Oak and pine are the most common and second most common genera in these plots, respectively (Table S1).

Soil Analyses. We collected two soil samples to a depth of 10 cm in each of four locations (0, 10, 20, and 30 m from the forest's edge) in each plot (n = 8 samples per plot) along a transect perpendicular to the center of the forest edge using a 5-cm-diameter bulk density soil corer. Roots and rocks were separated from the soil using a 2-mm sieve. The dry soil mass of each soil sample was estimated from the percentage change in soil mass of a 10-g subsample after it was dried to a constant weight at 65 °C. Dry root biomass was also quantified by drying to a constant weight at 65 °C. Rock volume, which was determined using a water displacement method, was subtracted from the volume of the soil core to calculate soil bulk density. Sieved soil samples were homogenized by plot and sampling location (n = 2 per sampling location in each plot), and C and N contents were determined using a CE Elantech NC2500 CN Analyzer (CE Elantech).

Forest Mensuration. Within each plot, the diameter at breast height (DBH) and species were recorded for every living tree larger than 5 cm DBH, and the location of each tree was mapped using a coordinate system. The BA of each tree was calculated following

$$BA = \pi \times \left(\frac{DBH}{2}\right)^2. \quad [1]$$

Forest BA of each forest segment (see below) was calculated for each plot by summing the BA values of the trees measured within each forest segment.

We collected two 5-mm tree cores (90° apart from one another) from each oak tree larger than 10 cm DBH in each plot. In addition, for one-half of the plot area, we collected cores from every tree larger than 10 cm DBH, regardless of genus. Tree cores were extracted from each tree 1.4 m above the ground. In total, 408 cores were collected ($n = 2$ cores per tree × 204 trees). Dried and mounted cores were sanded to a flat surface using successively finer sandpaper grits from 120 to 800.

Tree and Forest Growth. Tree cores were scanned using a high-resolution color scanner (Epson Perfection V700 Photo), and ring increments were measured to 0.001 mm using WinDENDRO 2012 (Regent Instruments, Inc.) image analysis software. Cross-dating was done visually with the statistical assistance of COFECHA (38).

To control for tree size effects on ring widths, raw tree ring measurements were converted to BAI following

$$BAI = \left(R_n^2\pi\right) - \left(R_{n-1}^2\pi\right), \quad [2]$$

where R_n is the radius of the tree at the end of year n, and R_{n-1} is the radius of the tree at the end of the previous year. The radius at the end of the most recent full year of growth (2014) for each tree was determined at the time of tree core sampling. For each tree, mean BAI was calculated from two cores collected from that tree; if both cores were not usable, only one core was used. Forest BAI of each forest segment (see below) was calculated for each plot by summing the BAI values of the trees cored within each plot.

Trees were binned into forest segments of 0–10, 10–20, and 20–30 m from the forest's edge to facilitate quantification of edge effects on stem density, BA, and BAI. Forest BA and BAI of each forest segment were calculated by summing BA and BAI across all trees within each segment.

We used the line-intercept method to quantify patterns in CWD between the forest's edge and interior [e.g., the work by Keller et al. (39)]. Seven 20-m transects running parallel to the forest's edge at 5-m intervals from 0 to 30 m from the forest's edge were established in each plot using measuring tapes. All CWD larger than 2 cm in diameter that intersected each transect was measured using calipers. The cross-sectional area of CWD was calculated from diameter measurements and summed for each transect.

Climate Data. We used historical climate records to isolate climate drivers of interannual variability in tree and forest growth between 1990 and 2014. Climate records were obtained for Boston, Massachusetts from the National Climate Data Center. Climate variables include minimum, mean, and maximum air temperature and precipitation at daily, monthly, and seasonal timescales and Palmer Drought Severity Index at monthly and seasonal timescales. One plot had many trees within 10 m of the forest's edge that were too young to have a time series that extended back to 1990, and therefore, for this plot, we only used data back to 2004.

We used statistically downscaled coupled Atmosphere–Ocean General Circulation Models climate projections from the CMIP5 (25) to estimate a first approximation of potential changes in spatial patterns of forest growth with proximity to the edge under the Intergovernmental Panel on Climate Change RCP 4.5 and RCP 8.5 scenarios (40). Model ensemble simulations (Table S2) were retrieved for the period 2080–2099 for 242 1/8°-grid cells encompassing southern New England (from 41.4375° N to 42.6875° N and from 73.4375° W to 70.8125° W).

We used our plot-level results to quantify the C implications of forest fragmentation at the landscape and regional scales of southern New England (Massachusetts, Connecticut, and Rhode Island), because the climate and species composition of the forest fragments used in this study are representative of much of the forest in this region (Fig. S1 and Table S5). Using ArcGIS with the 2011 NLCD 30-m resolution land cover layer (26), we created buffers to quantify the forest area within 10 and 20 m of the forest's edge. The NLCD uses the Anderson Land Cover Classification System to define four forest categories, which we consolidated into one.

Forest C density (megagrams C hectare^{-1}) and aboveground net primary productivity (ANPP) were obtained for southern New England using the Carbon OnLine Estimator (COLE) Tool [COLE v. 3.0; accessed October of 2016; www.ncasi2.org/GCOLE3/gcole.shtml (18)], which is a web suite of applications that uses FIA plot-level data to generate a range of user-defined forestry statistics and C estimates (33, 41). We use the variables "Carbon–Aboveground Live Tree" and "Biomass–Sound Annual Growth" for C density and ANPP, respectively. The COLE output includes means, sample size, and SE. We assume that these C densities are representative of the forest interior (defined here as >20 m from the forest's edge). To quantify C density within segments of 0–10 and 10–20 m from the forest's edge, we apply our field data characterizing the relative (i.e., percentage) change in BA from the forest's edge to interior. We use the same approach for quantifying forest growth (i.e., BAI) within segments of 0–10 and 10–20 m from the forest's edge.

BA Only Plots. In addition to the data collected from the "core plots" described above, during the summer of 2016, we quantified relative changes in BA between 0 and 40 m from the forest edge in 13 plots across eastern and central Massachusetts. Transects consisting of four 10-m fixed radius semicircular plots extending 0–40 m from the forest edge were used to efficiently quantify patterns in BA. This approach requires substantially less time than a full census and coring of trees in a plot but provides good estimates of relative changes in BA between the forest edge and interior that are highly correlated with the complete survey approach described above for our core plots ($r^2 = 0.91$; $P = 0.003$). These plots include a range of forest types and edge characteristics (Table S4) and are intended to compliment data from the core plots and broaden the scope of this study.

Statistical Analyses. All statistical analyses were conducted in R, version 3.0.2 (R Core Team). Forest edge effects on soil C, N, and bulk density; CWD; BA; and BAI were quantified using linear mixed effects models [lme function (42)] with forest segment (i.e., 0- to 10-, 10- to 20-, and 20- to 30-m segments from the forest's edge) or transect distance from edge in the case of CWD as the fixed effect and plot as the random effect. The 10-y mean BAI (2005–2014) of each forest segment was used to compare forest growth rates across forest segments. Although this approach does not account for changes in forest growth associated with mortality during this period, it is appropriate for quantifying relative changes in forest growth, because we do not find evidence of differences in CWD and by inference, mortality rates across forest segments (*Results and Discussion*). Climate drivers of interannual variability in the mean forest growth for each forest segment across all plots were quantified using multiple linear regression analyses. Unless otherwise indicated, all values reported are means and SE. An rms approach was used to propagate uncertainty of COLE and field data for each variable scaled to the landscape level.

ACKNOWLEDGMENTS. This research was conducted on land owned by Mass Audubon and the City of Lynn, Massachusetts, and we are grateful for assistance. We thank Conor Gately, Brady Hardiman, Ramona Hihn, Gabriela Jackson, Ian Smith, and Andrew Trlica for their help in collecting data; Roger Wrubel and the staff of Mass Audubon for assistance with site selection; and Jonathan Thompson for his feedback on this research. This research was supported primarily by National Oceanic and Atmospheric Administration Grant NA14OAR4310179, with additional support from US National Science Foundation Career Award DEB-1149471 and NASA Grants NNX12AM82G and NNH13CK02C.

1. Pan Y, et al. (2011) A large and persistent carbon sink in the world's forests. *Science* 333(6045):988–993.
2. Houghton RA (2010) How well do we know the flux of CO2 from land-use change? *Tellus B Chem Phys Meteorol* 62(5):337–351.
3. Arora VK, Boer GJ (2010) Uncertainties in the 20th century carbon budget associated with land use change. *Glob Chang Biol* 16(12):3327–3348.
4. Tian H, et al. (2016) The terrestrial biosphere as a net source of greenhouse gases to the atmosphere. *Nature* 531(7593):225–228.
5. Williams M (2006) *Deforesting the Earth: From Prehistory to Global Crisis, An Abridgement* (Univ Chicago Press, Chicago).
6. Haddad NM, et al. (2015) Habitat fragmentation and its lasting impact on Earth's ecosystems. *Sci Adv* 1(2):e1500052.
7. Weathers KC, Cadenasso ML, Pickett STA (2001) Forest edges as nutrient and pollutant concentrators: Potential synergisms between fragmentation, forest canopies, and the atmosphere. *Conserv Biol* 15(6):1506–1514.
8. Matlack GR (1993) Microenvironment variation within and among deciduous forest edge sites in the eastern United States. *Biol Conserv* 66:185–194.
9. Remy E, et al. (2016) Strong gradients in nitrogen and carbon stocks at temperate forest edges. *For Ecol Manage* 376:45–58.
10. Laurance WF (1997) Biomass collapse in Amazonian forest fragments. *Science* 278(5340):1117–1118.

11. Chen J, Franklin JF, Spies TA (1992) Vegetation responses to edge environments in old-growth douglas-fir forests. *Ecol Appl* 2(4):387–396.
12. Jonsson MT, et al. (2007) Eighteen years of tree mortality and structural change in an experimentally fragmented Norway spruce forest. *For Ecol Manage* 242(2–3):306–313.
13. Chaplin-Kramer R, et al. (2015) Degradation in carbon stocks near tropical forest edges. *Nat Commun* 6:10158.
14. Chen J, et al. (2004) A working framework for quantifying carbon sequestration in disturbed land mosaics. *Environ Manage* 33(Suppl 1):210–221.
15. Laurance WF, Bruce Williamson G (2001) Positive feedbacks among forest fragmentation, drought, and climate change in the Amazon. *Conserv Biol* 15(6):1529–1535.
16. Dyer JM (2006) Revisiting the deciduous forests of eastern North America. *Bioscience* 56(4):341–352.
17. Oswalt SN, Smith WB, Miles PD, Pugh SA (2014) *Forest Resources of the United States, 2012: A Technical Document Supporting the Forest Service 2015 Update of the RPA Assessment*, General Tech Rep WO-91 (US Department of Agriculture Forest Service, Washington, DC).
18. Van Deusen P, Heath LS *COLE Web Application Suite. NCASI and USDA Forest Service, Northern Research Station*. Available at www.ncasi2.org/COLE/. Accessed October 3, 2016.
19. Meadows JS, Goelz JCG (2002) Fourth-year effects of thinning on growth and epicormic branching in a red oak-sweetgum stand on a minor stream bottom site in west-central Alabama. *Proceedings of the Eleventh Biennial Southern Silvicultural Research Conference*, ed Outcalt KW (US Department of Agriculture, Forest Service, Southern Research Station, Asheville, NC), pp 201–208. General Technical Report SRS-48.
20. Briber BM, et al. (2015) Tree productivity enhanced with conversion from forest to urban land covers. *PLoS One* 10(8):e0136237.
21. Mcdonald R, Urban DL (2004) Forest edges and tree growth rates in the North Carolina piedmont. *Ecology* 85(8):2258–2266.
22. Ziter C, Bennett EM, Gonzalez A (2014) Temperate forest fragments maintain aboveground carbon stocks out to the forest edge despite changes in community composition. *Oecologia* 176(3):893–902.
23. Martin-Benito D, Pederson N (2015) Convergence in drought stress, but a divergence of climatic drivers across a latitudinal gradient in a temperate broadleaf forest. *J Biogeogr* 42(5):925–937.
24. Tang G, Beckage B, Smith B, Miller PA (2010) Estimating potential forest NPP, biomass and their climatic sensitivity in New England using a dynamic ecosystem model. *Ecosphere* 1(6):art18.
25. Taylor KE, Stouffer RJ, Meehl GA (2012) An overview of CMIP5 and the experiment design. *Bull Am Meteorol Soc* 93(4):485–498.
26. Homer CG, et al. (2015) Completion of the 2011 National Land Cover Database for the conterminous United States-Representing a decade of land cover change information. *Photogramm Eng Remote Sensing* 81(5):345–354.
27. Woodbury PB, Smith JE, Heath LS (2007) Carbon sequestration in the U.S. forest sector from 1990 to 2010. *For Ecol Manage* 241(1–3):14–27.
28. Thompson J, et al. (2013) *Changes to the Land: Four Scenarios for the Future of the Massachusetts Landscape*. Available at harvardforest.fas.harvard.edu/changes-to-the-land. Accessed May 3, 2016.
29. Smith FW, Long JN (2001) Age-related decline in forest growth: An emergent property. *For Ecol Manage* 144(1–3):175–181.
30. Urbanski S, et al. (2007) Factors controlling CO 2 exchange on timescales from hourly to decadal at Harvard Forest. *J Geophys Res* 112(G2):1–25.
31. Laurance WF, Ferreira LV, Merona JMR, Laurance SG (1998) Rain forest fragmentation and the dynamics of Amazonian tree communities. *Ecology* 79(6):2032–2040.
32. Smith P, et al. (2014) Agriculture, forestry and other land use (AFOLU). *Climate Change 2014: Mitigation of Climate Change*, eds Edenhofer O, et al. (Cambridge University Press, New York), pp 811–922.
33. Heath LS (2013) Using FIA data to inform United States forest carbon national-level accounting needs: 1990-2010. *Long-Term Silvicultural and Ecological Studies Results for Science and Management*, eds Camp AE, Irland LC, Carroll CJW (Yale University School of Forestry and Environmental Studies Global Institute of Sustainable Forestry, New Haven, CT), Vol 2, pp 149–161. GISF Research Paper 013.
34. Goodale CL, et al. (2002) Forest carbon sinks in the northern hemisphere. *Ecol Appl* 12(3):891–899.
35. Luyssaert S, et al. (2007) CO 2 balance of boreal, temperate, and tropical forests derived from a global database. *Glob Chang Biol* 13(12):2509–2537.
36. National Climatic Data Center (2014) *National Oceanic and Atmospheric Administration*. Available at https://www.ncdc.noaa.gov. Accessed May 1, 2014.
37. Jeon SB, Olofsson P, Woodcock CE (2014) Land use change in New England: A reversal of the forest transition. *J Land Use Sci* 9(1):105–130.
38. Holmes RL (1983) Computer-assisted quality control in tree-ring dating and measurement. *Tree-Ring Bulletin* 43:69–78.
39. Keller M, Palace M, Asner GP, Pereira R, Silva JNM (2004) Coarse woody debris in undisturbed and logged forests in the eastern Brazilian Amazon. *Glob Chang Biol* 10(5):784–795.
40. Collins M, et al. (2013) Long-term climate change: Projections, commitments and irreversibility. *Climate Change 2013: The Physical Science Basis*, eds Stocker TF, et al. (Cambridge University Press, New York), pp 1029–1136.
41. Proctor P, Heath LS, Van Deusen PC, Gove JH, Smith JE (2002) COLE: A Web-based tool for interfacing with forest inventory data. *Proceedings of the Fourth Annual Forest Inventory and Analysis Symposium*, eds McRoberts RE, Reams GA, Van Deusen PC, McWilliams WH, Cieszewski CJ (US Department of Agriculture, Forest Service, North Central Research Station, St. Paul), pp 167–172. General Technical Report NC-252.
42. Pinheiro J, Bates D, DebRoy S, Sarkar D (2012) nlme: Linear and nonlinear mixed effects models. R package version 3.1-105.

Supporting Information

Reinmann and Hutyra 10.1073/pnas.1612369114

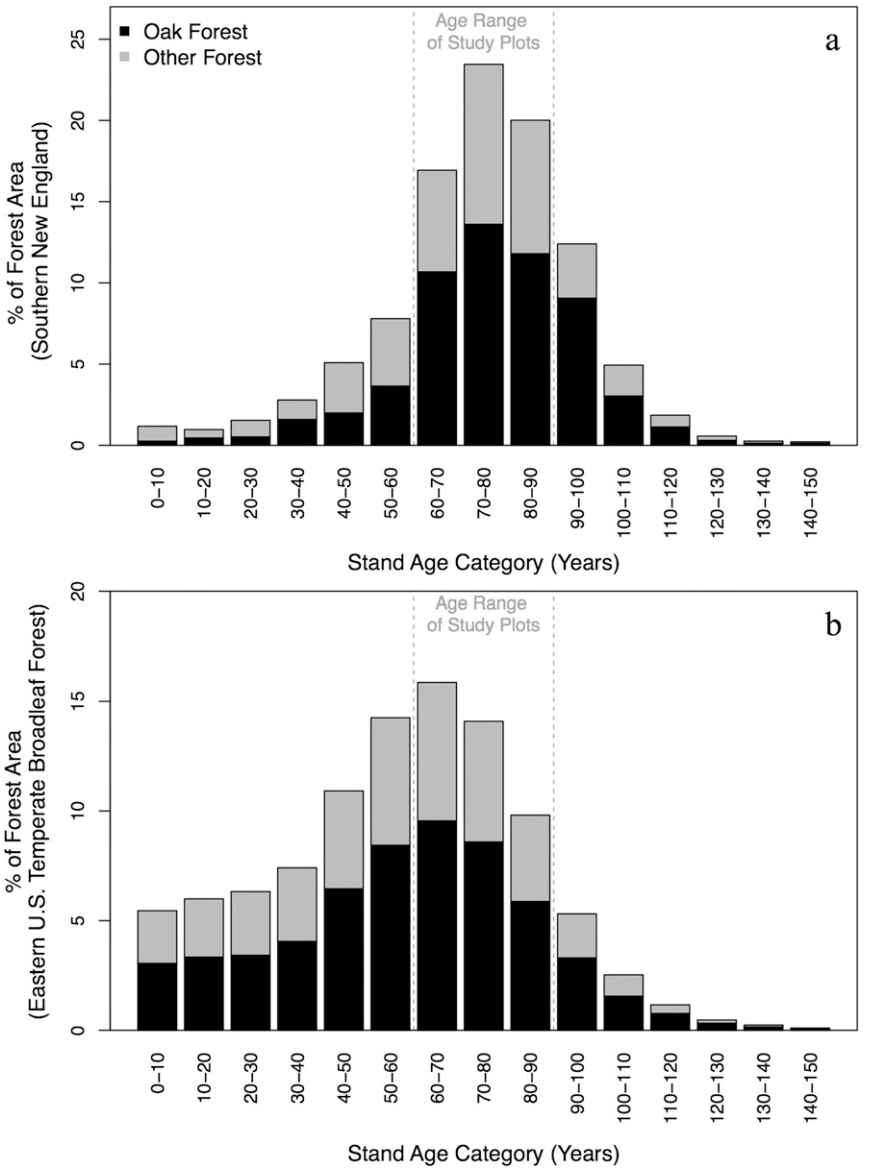

Fig. S1. Forest stand age distribution and the proportion of each age category made up of oak and other forest types for forests in (*A*) southern New England and (*B*) the eastern United States temperate broadleaf forest (states north of Florida and east of the Mississippi River). Oak forests are ~60% of the forest area across both spatial domains. Data were compiled using the US FIA COLE Tool (18).

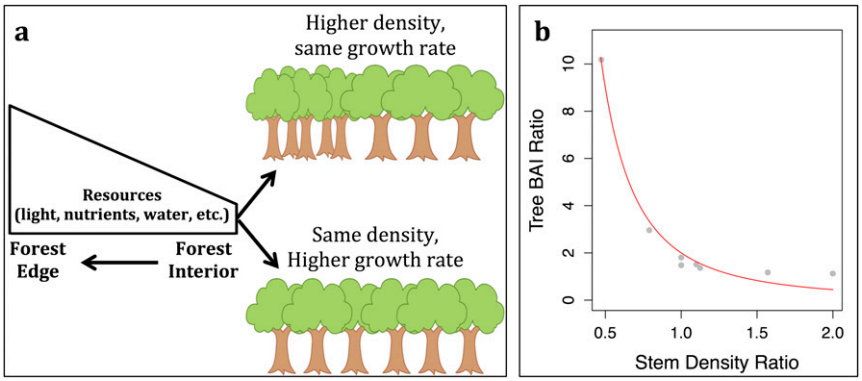

Fig. S2. Forest trajectories to higher overall forest growth and C storage with proximity to the forest's edge. (*A*) Conceptual diagram depicting the pathways through which higher resource availability near the forest's edge can influence growth of individual trees to increase rates of forest growth. (*B*) Observed relationship between relative tree stem density and mean tree BAI across study sites ($P < 0.01$; $n = 8$). Tree BAI and tree stem density ratios were calculated by dividing forest edge (0–10 m) mean tree BAI and stem density (>10 cm DBH), respectively, by the values of the same variable in the forest's interior (20–30 m).

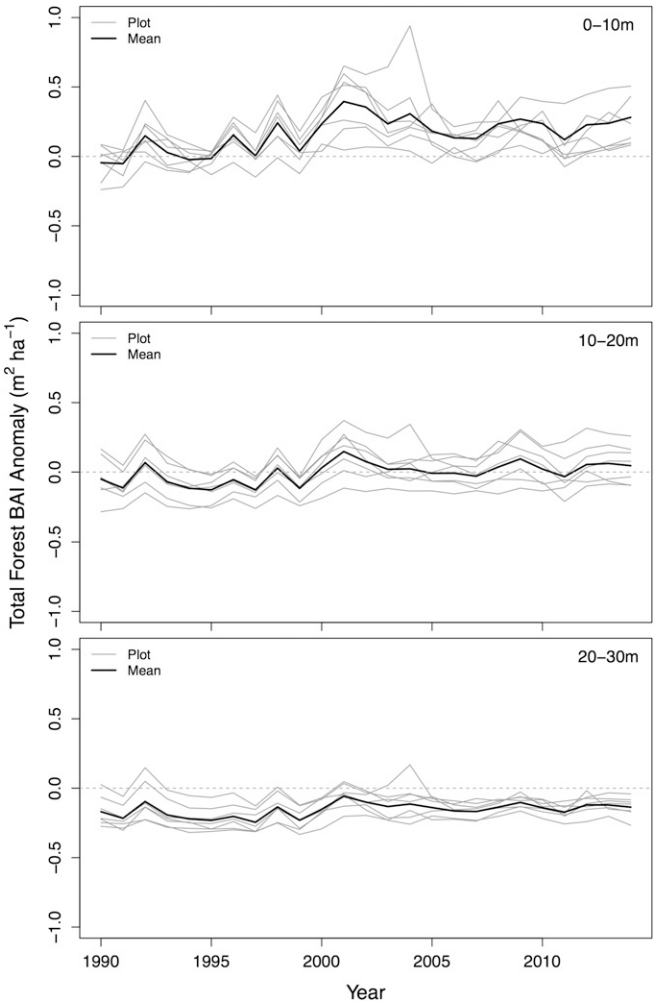

Fig. S3. Interannual patterns of total forest BAI anomalies for each 10-m forest segment between the edge and interior ($n = 8$ for each forest segment). Anomalies were calculated using mean BAI across forest segments as the reference value for each year.

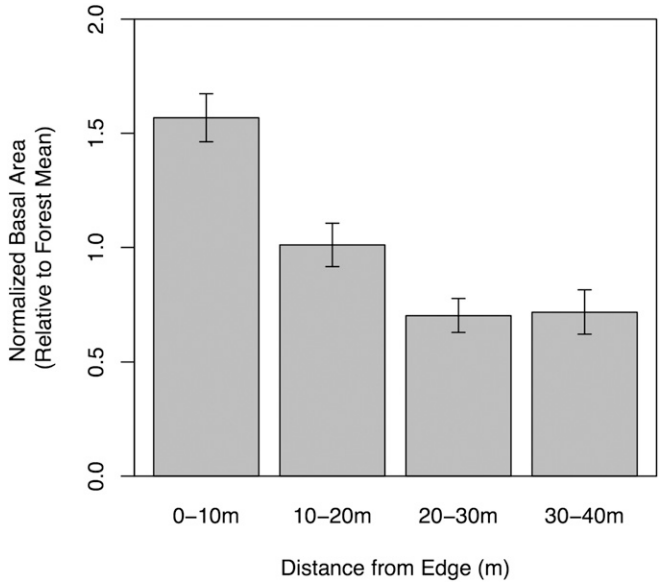

Fig. S4. Relative changes in BA between the forest edge and interior (slope = −0.286; $P < 0.001$) across 13 secondary plots established primarily to characterize edge effects on BA across a broad range of forest end edge types. BA is normalized to plot mean BA to account for inherent differences in BA across plots. Data represent means and SE of plots composed of oak forests, mixed broadleaf forests, and mixed broadleaf/conifer forests (Table S4).

Table S1. Relative BA of oak (*Quercus* spp.) and pine (*Pinus* spp.) in each plot and forest BAI growth enhancement in the forest segment 0–10 m from the edge compared with the interior (20–30 m)

Plot ID	Latitude	Longitude	Edge type	Percentage of total BA		Forest edge (0–10 m) growth enhancement (%)
				Pinus	*Quercus*	
Audubon A	42.40°N	71.19°W	Meadow	33.2	49.9	56.7
Audubon B	42.40°N	71.19°W	Meadow	14.3	60.8	189.6
Audubon C	42.40°N	71.19°W	Meadow	33.0	46.5	48.5
Audubon D	42.40°N	71.19°W	Residential	1.8	75.7	70.9
Audubon E	42.40°N	71.19°W	Residential	1.9	88.0	52.2
Audubon F	42.40°N	71.19°W	Residential	0.9	87.2	102.4
Lynn A	42.50°N	70.98°W	Residential	0.0	98.9	76.4
Lynn B	42.50°N	70.98°W	Residential	3.9	91.6	114.2

Latitude and longitude are approximate, because plots were located on or adjacent to private property.

Table S2. CMIP5 models used in this study

Modeling center (or group)	Institute identification	Model name
Commonwealth Scientific and Industrial Research Organization and Bureau of Meteorology, Australia	CSIRO-BOM	ACCESS1.0 ACCESS1.3
Beijing Climate Center, China Meteorological Administration	BCC	BCC-CSM1.1 BCC-CSM1.1(m)
Canadian Centre for Climate Modeling and Analysis	CCCMA	CanESM2 CanCM4 CanAM4
University of Miami–Rosenstiel School of Marine and Atmospheric Science	RSMAS	CCSM4(RSMAS)
National Center for Atmospheric Research	NCAR	CCSM4
Community Earth System Model Contributors	NSF-DOE-NCAR	CESM1(BGC) CESM1(CAM5) CESM1(CAM5.1,FV2) CESM1(FASTCHEM) CESM1(WACCM)
Centre National de Recherches Météorologiques/Centre Européen de Recherche et Formation Avancée en Calcul Scientifique	CNRM-CERFACS	CNRM-CM5 CNRM-CM5-2
Commonwealth Scientific and Industrial Research Organization in collaboration with Queensland Climate Change Centre of Excellence	CSIRO-QCCCE	CSIRO-Mk3.6.0
National Oceanic and Atmospheric Administration Geophysical Fluid Dynamics Laboratory	NOAA GFDL	GFDL-CM2.1 GFDL-CM3 GFDL-ESM2G GFDL-ESM2M GFDL-HIRAM-C180 GFDL-HIRAM-C360
Institute for Numerical Mathematics	INM	INM-CM4
Institut Pierre-Simon Laplace	IPSL	IPSL-CM5A-LR IPSL-CM5A-MR IPSL-CM5B-LR
Japan Agency for Marine-Earth Science and Technology, Atmosphere and Ocean Research Institute (The University of Tokyo), and National Institute for Environmental Studies	MIROC	MIROC-ESM MIROC-ESM-CHEM
Atmosphere and Ocean Research Institute (The University of Tokyo), National Institute for Environmental Studies, and Japan Agency for Marine-Earth Science and Technology	MIROC	MIROC4h MIROC5
Max Planck Institut für Meteorologie (Max Planck Institute for Meteorology)	MPI-M	MPI-ESM-MR MPI-ESM-LR MPI-ESM-P
Meteorological Research Institute	MRI	MRI-AGCM3.2H MRI-AGCM3.2S MRI-CGCM3 MRI-ESM1
Norwegian Climate Centre	NCC	NorESM1-M NorESM1-ME

Table S3. Forest statistics derived from NLCD 2011 and FIA data for forest area and biomass/growth values, respectively

State	Forest area (ha)	Forest <10 m of edge (ha)	Forest <20 m of edge (ha)	Forest aboveground biomass (Tg C)	Forest ANPP (Tg C y^{-1})
Connecticut	803,556	80,475 (10.0%)	148,714 (18.5%)	67.2 ± 0.8	1.9 ± 0.12
Massachusetts	1,259,041	118,248 (9.4%)	218,297 (17.3%)	101.0 ± 2.2	2.6 ± 0.11
Rhode Island	157,936	15,105 (9.6%)	27,988 (17.8%)	12.1 ± 0.5	0.3 ± 0.04
Southern New England	2,220,533	213,828 (9.6%)	394,999 (17.8%)	180.2 ± 2.9	4.9 ± 0.18

Data are for southern New England and each of three states that make up this region. Proportions of forest area within 10 and 20 m of the forest edge are indicated in parentheses. Forest edge values are in parentheses. Biomass/growth data are state and region means with SE.

Table S4. Sample size associated with each forest type and edge characteristic of plots used for measuring only BA (BA only; $n = 13$) and BA, forest growth, CWD, and soil variables (core plots; $n = 8$)

	Plot type	
Plot parameter	BA only	Core plots
Edge type		
Meadow	5	3
Residential lawn	1	5
Road	2	0
Power line right of way	3	0
Abandoned golf course	2	0
Forest type		
Oak	5	6
Mixed broadleaf	6	0
Mixed broadleaf/conifer	2	2

Table S5. Mean maximum air temperature during June and July for cities across southern New England

	Mean maximum temperature (degrees Celsius)	
City	June	July
Boston, MA	24.4	27.4
Hartford, CT	26.4	29.2
Lowell, MA	25.9	29.1
New Haven, CT	25.2	28.1
North Adams, MA	24.6	26.9
Providence, RI	25.3	28.2
Worcester, MA	23.4	26.1
Southern New England	25.0	27.8

Data are from the National Oceanic and Atmospheric Administration Northeast Regional Climate Center (climodtest.nrcc.cornell.edu/).